Inverse freezing in the Hopfield fermionic Ising spin glass

S. G. Magalhaes[*] and C. V. Morais

Departamento de Fisica, Universidade Federal de Santa Maria, 97105-900 Santa Maria, RS, Brazil

F. M. Zimmer

Departamento de Física, Universidade do Estado de Santa Catarina, 89223-100 Joinville, SC, Brazil

In this work we studied the Hopfield fermionic spin-glass model which allows interpolating from trivial randomness to a highly frustrated regime. Therefore, it is possible to investigate whether or not frustration is an essential ingredient which would allow this magnetic-disordered model to present naturally inverse freezing by comparing the two limits, trivial randomness and highly frustrated regime, and how different levels of frustration could affect such unconventional phase transition. The problem is expressed in the path-integral formalism where the spin operators are represented by bilinear combinations of Grassmann variables. The grand canonical potential is obtained within the static approximation and one-step replica symmetry-breaking scheme. As a result, phase diagrams temperature versus the chemical potential are obtained for several levels of frustration. Particularly, when the level of frustration is diminished, the reentrance related to the inverse freezing is gradually suppressed.

I. INTRODUCTION

There is current interest (see, for instance, Refs. [1–7]) in studying inverse transitions, melting or freezing, motivated by the quite unconventional situation present in such transitions in which the ordered phase is more entropic than the disordered one.[8] This apparent counter-intuitive transition has become even more interesting since there are now various physical systems displaying this kind of transition, as for example, magnetic films[9] and, particularly, high-T_c superconductors.[10] Therefore, the knowledge about which conditions are necessary for the existence of inverse transitions is a challenging issue.[11]

Among the proposed classical magnetic models which can show inverse transitions, the Blume Capel (BC) (Ref. [1]) and the Gathak-Sherrington (GS) (Refs. [1], [2], and [5]) models can be useful to clarify what would be such conditions. For instance, the phase diagram of the BC model[12] displays inverse melting with a phase transition from the ferromagnetic (FM) phase to the paramagnetic (PM) one when the temperature is decreased. However, in order to obtain inverse melting in the BC model, it is strictly necessary to impose in the problem the entropic advantage of the interacting state through parameter $r=l/k \geq 1$, where l and k are the degeneracy of ± 1 and 0 spins states, respectively.[1] In contrast with the BC model, the GS model[13]—which is similar to the BC model except that it has the spins couplings given as random Gaussian variables—shows naturally inverse freezing. In other words, there is a reentrant first-order boundary phase separating the spin glass (SG) and PM phases. However, there is no need of any entropic advantage of interacting states.[2,5] The previous discussion suggests that the randomness is responsible for producing naturally inverse freezing in the GS model as compared with the inverse melting case in the BC model. In fact, to be more precise, it seems that the presence of nontrivial form of randomness, which means frustration,[14] would be the essential ingredient which allows inverse freezing in the GS model with no need of entropic

advantage. That sets some questions: What is the actual role of nontrivial randomness to produce naturally inverse freezing? Is this natural inverse freezing robust when the level of frustration is diminished? Can models with trivial randomness present naturally inverse transitions?

The purpose of the present work is to investigate what is the actual role of frustration as a basic condition to produce naturally inverse freezing. That could be achieved by comparing two distinct situations, the trivial randomness and the highly frustrated regime, and also studying how natural inverse freezing would be affected when the level of frustration is varied. Therefore, the problem is not only to find a random magnetic model which presents naturally inverse freezing but also to get one which allows the level of frustration to vary. Quite recently, the fermionic Ising spin-glass (FISG) model[7] has been proposed as a model able to display naturally inverse freezing in a phase-diagram temperature versus the chemical potential μ. This model has the spin operators $\hat{S}_i^z$ given as bilinear combinations of creation and destruction fermionic operators which have four eigenstates, two of them nonmagnetic.[15–17] The spin-spin coupling J_{ij}, likewise the GS model, is a random variable which follows a Gaussian distribution. Indeed, the existence of inverse freezing in this model could be expected since there is a close relationship between the GS and the FISG models.[18] For instance, the partition function of these two models can be related by a mapping between the anisotropy constant D of the GS model and μ.[19]

The FISG model is also useful to examine how quantum effects, included by the presence of a transverse field Γ (Refs. [16] and [20]) can affect inverse freezing. In Ref. [7], it has been shown that, when Γ is increased, the reentrance in the SG/PM first-order boundary phase in the phase-diagram temperature T versus the chemical potential μ gradually disappears. This scenario also suggests that Γ in the FISG model plays the opposite role of the rather artificial parameter r in the BC model discussed in Ref. [1]. Nevertheless, the FISG

model, in its original form with Gaussian random couplings, is a strongly frustrated model. Therefore, it is not possible to investigate in this model how the change in the level of frustration could affect the inverse freezing.

An alternative route to accomplish the previously mentioned investigation would be to use the FISG model in a version in which one could adjust the level of frustration. In that sense, the classical Hopfield spin glass[21,22] can be quite useful. In this model, the interactions J_{ij} between classical Ising spins are given below

$$J_{ij} = \frac{J}{2N} \sum_{\varrho=1}^{p} \xi_i^{\varrho} \xi_j^{\varrho}, \tag{1}$$

where $\xi_i^{\varrho} = \pm 1$ (i or $j = 1, 2, \ldots, N$, where N is the number of sites) are independent random distributed variables. This type of interaction has been intensively used to study complex systems.[21] There are clearly two extreme cases for the classical Hopfield Ising spin-glass model. When $p=1$, it becomes the Mattis model,[23] which is a well-known example of trivial randomness.[14] The second one is when $p \rightarrow \infty$. In that limit, the thermodynamics corresponds to the strongly frustrated regime given by a random Gaussian distributed J_{ij}.[24] In particular, the replica symmetric mean-field solution of the classical Hopfield spin-glass model[22] can provide a useful method for the purposes of the present work. It is described in terms of two order parameters, the usual spin glass q and $m_{\varrho} = \frac{1}{N} \sum_{i=1}^{N} \xi_i^{\varrho} \langle S_i \rangle$ which indicates the presence of Mattis states that have a thermodynamics similar to the usual ferromagnetism.[21,22] Most important, there is a parameter called here degree of frustration, $a = p/N$ which allows controlling the level of frustration in the theory. It is important to remark that there is a particular value a_c which for $a > a_c$ the effects of frustration are dominant.[21,22] As a consequence, it is possible to interpolate the thermodynamics from the trivial randomness ($a = 0$) to the strongly frustrated regime ($a > a_c$).

Therefore, to answer the questions arisen previously, we use the Hopfield Fermionic Ising spin-glass (HFISG) model. In this case, the spin operators $\hat{S}_i^z$ are defined as the FISG model but the random spin coupling J_{ij} is given as Eq. (1). The partition function is obtained in the functional integral formalism using Grassmann fields where the disorder is treated with the replica method.[25] The problem can be reduced to a one-site problem by using a similar procedure to solve the classical Hopfield spin glass[21,22] within the static approximation (SA) (Ref. 26) and one-step replica symmetry breaking (1S-RSB).[27] It should be remarked that in the HFISG model, as the FISG one,[15,17,20,28] the replica diagonal component of the SG order parameter $q_{\alpha\alpha}$ appears as an additional order parameter to be solved with the others. Particularly, this order parameter represents the spin self-interaction that has an imaginary time dependence for quantum SG models.[26,29] However, the spin operators $\hat{S}_i^z$ commute with the Hamiltonian operators for the present HFISG model. Consequently, the $q_{\alpha\alpha}$ has no dynamic, which means that the SA is exact in the present work.[15,16]

One important point in the present work is how to locate first-order boundaries phases found for different degrees of

frustration. The criterion adopted here follows closely that one suggested in Ref. 30 for the classical GS model. Hence, we selected, from the set of spin-glass solutions in the transition that one which meets continuously with the spin-glass solution for small value of the chemical potential μ. In fact, that corresponds to the largest spin-glass order parameter which gives the lowest grand canonical potential (see also the discussion in Ref. 31). Then, by equating the grand canonical potential of the spin-glass and paramagnetic solutions, the first-order boundary phase is located.

The use of the 1S-RSB scheme also deserves some remarks since our main interest is to obtain boundaries of phase transitions. It has been found in previous works[2,5,7] that the use of the RSB schemes in GS or FISG models essentially preserves the reentrance in the SG/PM first-order boundary phase associated to the inverse freezing. There are only small differences which appear mainly at very low temperatures. Even so, for the HFISG model, we decided to use 1S-RSB scheme to check for intermediated values of a whether or not these differences will remain unimportant. Moreover, we also analyzed the stability of the RS solutions for the sake of completeness of the work.

This paper is structured as follow: in Sec. II, we derived the thermodynamics and the set of coupled equations for the saddle-point order parameters. In Sec. III, phase-diagrams temperature versus the chemical potential are presented for several values of a. The entropy behavior as function of temperature and the grand canonical potential as function of chemical potential are also discussed. Finally, Sec. IV is reserved to conclusions.

II. MODEL

The Hamiltonian considered here is a HFISG model

$$\hat{H} = -\sum_{ij} J_{ij} \hat{S}_i^z \hat{S}_j^z, \tag{2}$$

where J_{ij} is given in Eq. (1) and the random ξ_i^{ϱ} follows the distribution

$$P(\xi_i) = \frac{1}{2} \delta_{\xi_i^{\varrho}, +1} + \frac{1}{2} \delta_{\xi_i^{\varrho}, -1}. \tag{3}$$

In this model, $\hat{S}_i^z = \frac{1}{2}[\hat{n}_{i\uparrow} - \hat{n}_{i\downarrow}]$ is the spin operator, with $\hat{n}_{i\sigma} = c_{i\sigma}^{\dagger} c_{i\sigma}$ as the number operator, $c_{i\sigma}^{\dagger}(c_{i\sigma})$ are fermions creation (destruction) operators and $\sigma = \uparrow$ or $\downarrow$ indicate the spin projections.

The partition function in the grand canonical ensemble is given in the Lagrangian path integral formalism where the spin operators are represented as bilinear combinations of anticommuting Grassmann fields (ϕ, ϕ^*) (Ref. 32)

$$Z\{\mu\} = \int D(\phi^* \phi) e^{A\{\mu\}}, \tag{4}$$

where

$$A(\mu) = \int_0^\beta d\tau \left\{ \sum_{j,\sigma} \phi_{j\sigma}^*(\tau)\left(-\frac{\partial}{\partial \tau} + \mu\right)\phi_{j\sigma}(\tau) \right.$$
$$\left. - H[\phi^*(\tau),\phi(\tau)]\right\}, \tag{5}$$

where μ is the chemical potential and $\beta = 1/T$. $Z\{\mu\}$ is Fourier transformed in time which results in

$$Z\{\mu\} = \int D(\phi^*\phi)e^{A_\mu + A_{\mathrm{SG}}} \tag{6}$$

with

$$A_\mu = \sum_{j,\omega}\sum_\sigma \phi_{j\sigma}^\dagger(\omega)[i\omega + \beta\mu]\phi_{j\sigma}(\omega), \tag{7}$$

$$A_{\mathrm{SG}} = \sum_\Omega \sum_{ij} \beta J_{ij} S_i^z(\omega')S_j^z(-\omega') \tag{8}$$

and

$$S_i^z(\omega') = \frac{1}{2}\sum_\omega\sum_\sigma \sigma_s \phi_{i\sigma}^\dagger(\omega+\omega')\phi_{i\sigma}(\omega), \tag{9}$$

where μ is chemical potential, $\omega = (2m+1)\pi$, $\omega' = 2m\pi(m=0,\pm1,\ldots)$ are the Matsubara's frequencies and $\sigma_s = +(-)$ if $\sigma = \uparrow(\downarrow)$. In this work, the problem is analyzed within SA which considers only the term when $\omega' = 0$ in Eq. (9).[16,26,28,33]

The grand canonical potential is obtained by using the replica method

$$\beta\Omega = -\lim_{n\to 0} 1/(nN)(\langle\langle Z(n)\rangle\rangle_\xi - 1), \tag{10}$$

where $Z(n) \equiv Z^n$ and $\langle\langle\ldots\rangle\rangle_\xi$ means the configurational averaged over ξ. Thus

$$Z(n) = \prod_{\alpha=1}^n \int D(\phi_\alpha^*,\phi_\alpha)\exp[A_\mu^\alpha + A_{\mathrm{SG}}^{\alpha stat}], \tag{11}$$

where after using J_{ij} given in Eq. (1), the action A_{SG}^{stat} can be written as

$$A_{\mathrm{SG}}^{\alpha stat} = \frac{\beta J}{2N}\sum_{\varrho=1}^p\sum_{\alpha=1}^n\left(\sum_i \xi_i^\varrho S_i^\alpha\right)^2 - \frac{\beta Jp}{2N}\sum_i\sum_{\alpha=1}^n (S_i^\alpha)^2 \tag{12}$$

with α denoting the replica index and $S_i^\alpha \equiv S_i^\alpha(0)$.

The average over $Z(n)$ given in Eq. (11) is discussed in detail in Appendix A. In the present work, the 1S-RSB ansatz is adopted, in which the replica matrix $\{Q\}$ and the matrix $\{r\}$ are parametrized as

$$q_{\alpha\beta} = \begin{cases} \bar{q} & \text{if } \alpha = \beta \\ q_1 & \text{if } |\alpha - \beta| \le x \\ q_0 & \text{otherwise} \end{cases} \quad r_{\alpha\beta} = \begin{cases} \bar{r} & \text{if } \alpha = \beta \\ r_1 & \text{if } |\alpha - \beta| \le x \\ r_0 & \text{otherwise} \end{cases} \tag{13}$$

and order parameters m_1^α are invariant with respect to permutations of replicas: $m_1^\alpha = m$, where $\alpha = 1,\ldots,n$. Therefore, the parametrization in Eq. (13) is used in Eqs. (A8) and (A9). As

a consequence, the 1S-RSB grand canonical potential is found as

$$\beta\Omega = -\beta\mu + \frac{\beta^2 J^2 a}{2}(\bar{r}\bar{q} - (1-x)r_1 q_1 - xr_0 q_0)$$
$$+ \frac{a}{2x}\ln\frac{1 - \beta J[\bar{q} - q_1 + x(q_1 - q_0)]}{1 - \beta J(\bar{q} - q_1)}$$
$$- \frac{1}{2}\frac{\beta Jaq_0}{1 - \beta J[\bar{q} - q_1 + x(q_1 - q_0)]} + \frac{\beta Jm^2}{2}$$
$$+ \frac{a}{2} \times \ln[1 - \beta J(\bar{q} - q_1)] - \lim_{n\to 0}\frac{1}{n}\ln\langle\langle\Theta[(r),m,\xi]\rangle\rangle_\xi, \tag{14}$$

where

$$\Theta(\{r\},m,\xi) = \int \prod_\alpha^n D(\phi_\alpha^*,\phi_\alpha)$$
$$\times \exp\left[\frac{\beta^2 J^2 a}{2}\left[(\bar{r} - r_1 - 1/\beta J)\sum_{\alpha=1}^n (S^\alpha)^2\right]\right.$$
$$\times \exp\left[(r_1 - r_0)\sum_{l=1}^{n/x}\left(\sum_{\alpha=(l-1)x+1}^{lx} S^\alpha\right)^2\right]$$
$$\times \exp\left[r_0\left(\sum_{\alpha=1}^n S^\alpha\right)^2 + \beta J\sum_{\alpha=1}^n (\xi m S^\alpha)\right] \tag{15}$$

with $a = p/N$. The quadratic forms into the function $\Theta(\{r\},m,\xi)$ can be linearized by Hubbard-Stratonovich transformations where new auxiliary fields are introduced in the problem. Therefore, one has

$$\Theta[(r),m,\xi] = \int Dz\left\{\int Dv\left[\int Dw\right.\right.$$
$$\left.\left.\times \int D(\phi^*\phi)\exp\sum_{\omega\sigma} \phi_\sigma^*(\omega)G^{-1}(\omega)\phi_\sigma(\omega)\right]^x\right\}^{n/x} \tag{16}$$

with $Dy = \frac{dy e^{-y^2/2}}{\sqrt{2\pi}}$ ($y = z,v,w$) and

$$G^{-1}(\omega) = g^{-1}(\omega) + \bar{h}(z,v,w) + \beta J(\xi m). \tag{17}$$

The local spin-glass component of the random field $\bar{h}(z,v,w)$ is defined by

$$\bar{h}(z,v,w) = \beta J[\sqrt{ar_0}z + \sqrt{a(r_1 - r_0)}v + \sqrt{a(\bar{r} - r_1 - 1/\beta J)}w]. \tag{18}$$

The functional integral over the Grassmann variables, as well as the sum over the Matsubara's frequencies in Eq. (16), can be performed following closely the procedure given in Refs. 16 and 20. Finally, the grand canonical potential within 1S-RSB approximation can be written as
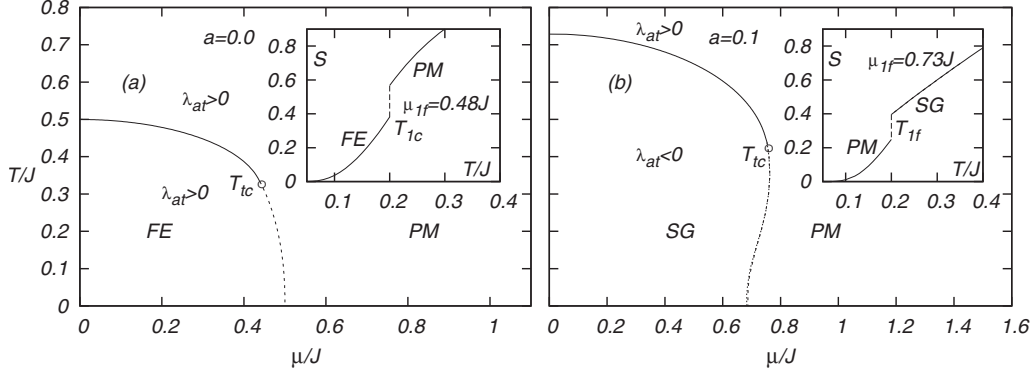
FIG. 1. Phase diagrams T/J versus μ/J for $a=0.0$ and $a=0.1$. In the phase diagrams, the full lines represent the second-order transition and the dashed lines represent the first-order transition. T_{tc} indicates the tricritical point. The insets show the entropy S versus T/J for specific values of μ/J in the first-order transition, where T_{1c} and T_{1f} represent the first-order transition between FE/PM and SG/PM phases, respectively.

$$\beta\Omega = \frac{\beta^2 J^2 a}{2}[\overline{rq} - (1-x)r_1 q_1 - x r_0 q_0] + \frac{\beta J m^2}{2}$$

$$-\frac{1}{2}\frac{\beta J a q_0}{1 - \beta J[\overline{q} - q_1 + x(q_1 - q_0)]} + \frac{a}{2}\ln[1 - \beta J(\overline{q} - q_1)]$$

$$+\frac{a}{2x}\ln\frac{1 - \beta J[\overline{q} - q_1 + x(q_1 - q_0)]}{1 - \beta J(\overline{q} - q_1)} - \beta\mu$$

$$-\frac{1}{x}\int Dz\left\langle\left\langle \ln\int Dv[2K(z,v|\xi)]^x \right\rangle\right\rangle_\xi, \qquad (19)$$

where

$$K(z,v|\xi) = \cosh\beta\mu + e^{\beta Ja/2[\beta J(\overline{r}-r_1)-1]}\cosh\overline{H}(z,v,\xi) \qquad (20)$$

and

$$\overline{H}(z,v|\xi) = \beta J[\sqrt{ar_0}z + \sqrt{a(r_1-r_0)}v + \xi m]. \qquad (21)$$

The set of equations for the order parameters m, q_0, q_1, $\overline{q}$, and the block size parameter x can be found from Eq. (19) using the saddle-point conditions.

In particular, the elements of matrix r are given by

$$r_0 = \frac{q_0}{\{1 - \beta J[\overline{q} - q_1 + x(q_1 - q_0)]\}^2}, \qquad (22)$$

$$r_1 - r_0 = \frac{q_1 - q_0}{[1 - \beta J(\overline{q} - q_1)]\{1 - \beta J[\overline{q} - q_1 + x(q_1 - q_0)]\}}, \qquad (23)$$

$$\overline{r} - r_1 = \frac{1}{\beta J[1 - \beta J(\overline{q} - q_1)]}. \qquad (24)$$

The average over ξ in the grand canonical potential can be done using the parity properties of the functions dependent on z and v. The entropy can also be obtained directly from the grand canonical potential.

The stability of the RS solution $q_{\alpha\beta}=q$, $r_{\alpha\beta}=r$ $(\alpha\neq\beta)$ is studied using the Almeida-Thouless analysis, in which the

condition for the stable RS solution $(\lambda_{at}>0)$ is obtained as[34]

$$\lambda_{at} = [1 + \beta J(q - \overline{q})]^2 - a(\beta J)^2 \int Dz$$

$$\times\left\{\frac{e^u\cosh H(r)}{K(r,\overline{r})} - \left[\frac{e^u\sinh H(r)}{K(r,\overline{r})}\right]^2\right\}^2 \qquad (25)$$

with $K(r,\overline{r}) = \cosh(\beta\mu) + e^u\cosh H(r)$ and

$$u = \frac{1}{2}\beta Ja[\beta J(\overline{r}-r)-1], \quad H(r) = \beta J\sqrt{arz} + \beta Jm. \qquad (26)$$

III. RESULTS

The numerical solutions for the coupled set for the saddle-point order parameters q_1, q_0, $\overline{q}$, and m are displayed in phase diagrams T/J versus μ/J given below for several values of the parameter a, where T is the temperature and J is defined in Eq. (1). For the numerical results, $J=1$ is used. The RS scheme for the order parameters is also calculated when $q_0=q_1\equiv q$. The stability of such solution is investigated by calculating the Almeida-Thouless eigenvalue λ_{AT} given in Eqs. (25) and (26). Such analysis shows that the PM solutions and Mattis states (FE) present $\lambda_{AT}>0$ while the SG ones have $\lambda_{AT}<0$. This result could indicate that it is necessary to use RSB schemes to locate more adequately the SG/PM first-order boundary phase. However, the results shown in Figs. 1 and 2 have found that, in such first-order boundary phase, the reentrance and, therefore, the inverse freezing are not essentially affected by the use of RS or 1S-RSB schemes similar to the FISG model.[7]

In Fig. 1, it is presented phase diagrams which illustrate two quite distinct situations concerning the degree of frustration. The first one $(a=0)$, which is shown in Fig. 1(a), corresponds to trivial randomness,[14] which means that there are no effects of frustration. In this phase diagram, for low T/J and small μ/J, one gets FE as solution. For higher T/J and/or larger μ/J, it is found the PM solution. For small μ/J, the boundary phase transition between FE and PM phase [called here $T_{2c}(\mu)$] is second order. However, when
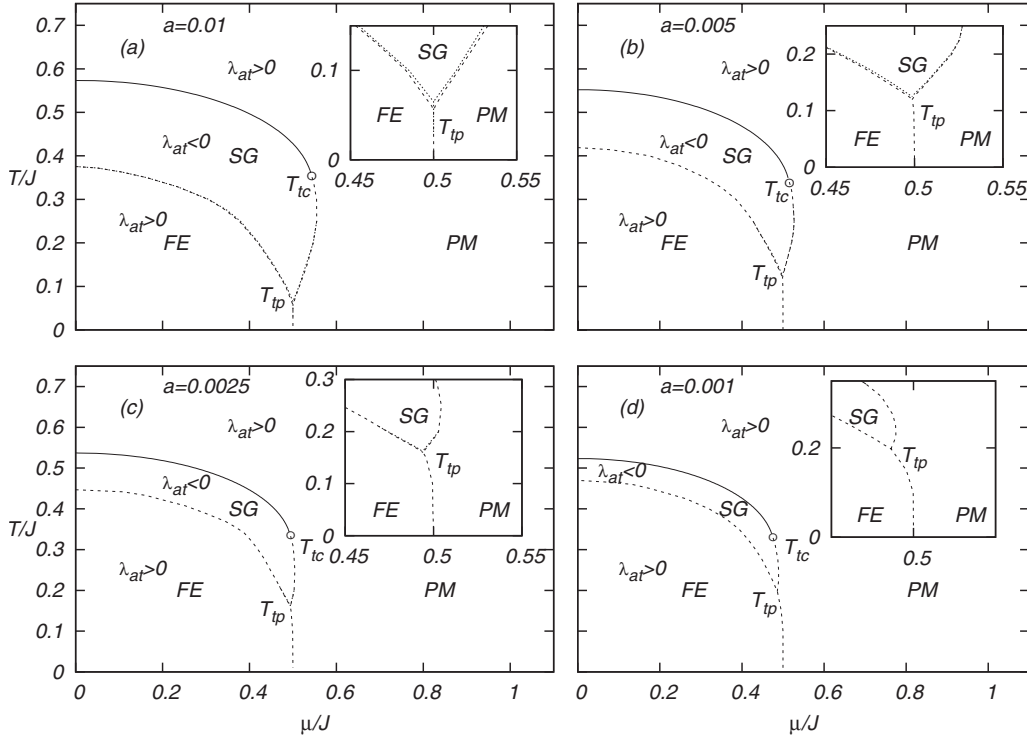
FIG. 2. Phase diagrams T/J versus μ/J for several low values of a. T_{tc} is a tricritical point and T_{tp} is a triple point. Dashed lines represent the first-order transition and solid lines represent the second-order transition. The insets show the location of the triple point in details. Close to the triple point, a small difference between the first-order boundary of the 1S-RSB (dotted lines) and RS (dashed lines) solutions can be seen in the insets.

μ/J increases, it appears a tricritical point located at $T_{tc}=J/3$ and $\mu_{tc}=0.438J$ (see Appendix B). Most important, there is no reentrance in the subsequent first-order part of the boundary phase transition $T_{1c}(\mu)$. In Fig. 1(b), the degree of frustration is increased ($a=0.1$) and, for that case, effects of frustration become dominant. Thus, the FE solution is replaced by a SG one in which, $m=0$, $\bar{q}\neq0$, $q_0\neq0$, and $q_1\neq0$ while the PM phase has $m=0$, $\bar{q}\neq0$, $q_0=0$, and $q_1=0$. The freezing temperature has also a second-order part $T_{2f}(\mu)$. As for the trivial randomness case, a tricritical point appears, with value $T_{tc}\approx0.438J$ and $\mu_{tc}\approx0.752J$ (see Appendix B). Nevertheless, the first order part of the freezing temperature $T_{1f}(\mu)$ now shows a reentrance which indicates the existence of inverse freezing, as it can be seen in the inset in Fig. 1(b), which displays the entropy as function of T/J. There, it is shown that entropy of the SG phase is larger than the PM one for that particular degree of frustration. It should be remarked that this phase diagram is quite similar to that one found for the FISG model.[7] The location of the boundaries phases in Fig. 1 has been checked in the limits $\mu=0$ and $T=0$ as it can be seen in Appendices B and C.

There is a more complex scenario as compared with that one described in Fig. 1(b) when $a\rightarrow0$. In Fig. 2(a) ($a=0.01$), the solution for the order parameters shows a phase diagram which illustrates this new scenario. For a small μ/J, when T/J is decreased, there is a second-order phase transition between the PM and SG phases. However, for even lower temperatures, there is another phase transition, which is now a first-order one, between the SG phase and FE region, which is given now by $m\neq0$, $\bar{q}\neq0$, $q_0\neq0$,

and $q_1\neq0$. For this particular value of a, SG and FE solutions occupy approximately equal sizes in the phase diagram. The freezing temperature has a similar behavior to that one found in Fig. 1(b). It has a second-order part $T_{2f}(\mu)$ for small μ, then it appears a tricritical point at $T_{tc}\approx0.366J$ and $\mu_{tc}\approx0.539J$ (see Appendix B). Below this point, $T_{1f}(\mu)$ presents a reentrance which allows, for an adequate constant μ, crossing from the SG phase to the PM one when the temperature is decreasing. Nonetheless, this first-order boundary phase has a complex nature. It appears a triple point at (T_{tp},μ_{tp}) where FE, PM, and SG phases coexist. Below this point, the first-order boundary phase $T_{1c}(\mu)$ displays no reentrance, as in the case $a=0$.

For smaller values of a, as shown in Figs. 2(b)–2(d), the region where FE solutions are found becomes increasingly larger than the SG one which is consistent with earlier results found in the classical Hopfield spin-glass model which displays, in a phase diagram T versus a, a dominance of the Mattis states when $a\rightarrow0$.[21] Even so, in this new situation, the location $T_{2f}(\mu)$ is not affected so much. However, the tricritical point is displaced for smaller and lower values of μ/J and T/J, respectively. In comparison, the triple point is displaced for smaller values of μ/J and higher values of T/J. As a consequence, $T_{1f}(\mu)$ and $T_{1c}(\mu)$ appear in a decreasing and increasing range of temperature, respectively. Nevertheless, most important, the reentrance in $T_{1f}(\mu)$ is gradually suppressed when $a\rightarrow0$. However, the inset in Fig. 2(d) shows that even when the level of frustration is very weak, and $T_{2f}(\mu)$ appears in a very short range of temperature, a reentrance in such first-order boundary phase is still preserved.
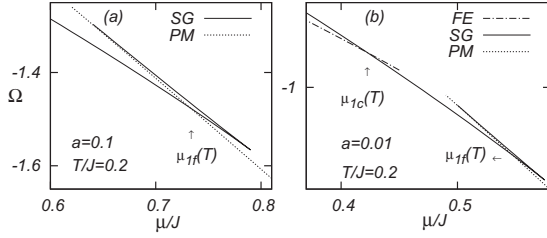
FIG. 3. Grand canonical potential Ω versus μ/J for $T/J=0.2$ and two values of $a=0.1$. The full, dotted, and dashed-dotted lines represent the Ω of SG, PM, and FE solutions, respectively.

The procedure to locate the first-order boundary lines in the previous phase diagrams is illustrated in Fig. 3, where the grand canonical potential versus μ/J is plotted for $T/J=0.2$. In Fig. 3, the set of multiple SG solutions is represented by branches of full lines, where the chosen SG solution is that one which meets continuously with the only one SG solution available for small values of μ/J. From that SG solution, the first-order boundary phase is obtained by equating the grand canonical potential of SG, PM, and FE solutions.

The corresponding behavior of the entropy as a function of T/J for the values of a used in Fig. 2 is shown in Fig. 4. This figure illustrates the gradual suppression of inverse freezing when $a \to 0$. For instance, in Fig. 4(a), the value of $\mu=0.53J$ is chosen to cross the reentrant first-order boundary phase in $T_{1f}(\mu)$ in Fig. 2(a). The figure shows that the entropy of SG phase is larger than the entropy of the PM one in the first-order transition which, as in the inset of Fig. 1(b), indicates the existence of inverse freezing. The same procedure has been adopted in Figs. 2(b)–2(d), values of μ are adjusted to be close to μ_{tp}. The result found in Fig. 2(b) is similar to that one found in Fig. 2(a). However, Fig. 2(c) displays the entropy behavior when $T_{1f}(\mu)$ and $T_{1c}(\mu)$ are now crossed. The first crossing is in the reentrant line transition $T_{1f}(\mu)$ giving an inverse freezing as in Figs. 2(a) and 2(b). The second one in $T_{1c}(\mu)$ gives a usual phase transition in which the PM phase is more entropic than the FE one, as already found in Fig. 1(a). In Fig. 2(d) the reentrance in $T_{1f}(\mu)$ is almost suppressed. Thus, for the chosen value of μ,

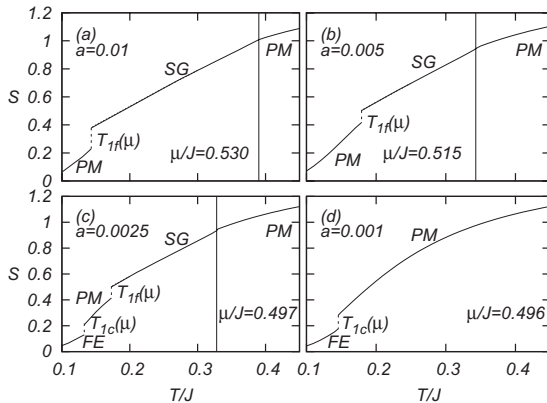

FIG. 4. Entropy S versus T/J for several values of a and μ/J. The labels $T_{1c}(\mu)$ and $T_{1f}(\mu)$ indicate the first-order transition between the FE/PM and SG/PM phases, respectively. The full vertical line indicates the second-order transition between SG/PM phases.

there is only one crossing in $T_{1c}(\mu)$ which gives the entropy behavior of a usual phase transition as that one found in Fig. 1(a).

IV. CONCLUSION

In the present work, it has been studied the HFISG model in which the random spin-spin coupling J_{ij}, instead of the usual Gaussian distribution, is given by Eq. (1). For this particular choice of J_{ij}, the problem can be treated in a mean-field framework which allows adjusting the level of frustration. Therefore, it is possible to study not only the existence of a natural inverse freezing in the limits of trivial randomness and strong frustration but also how changing the level of frustration could affect such transition. In this approach, within 1S-RSB scheme, besides the replica nondiagonal SG orders parameters q_0, q_1, and the block size parameter x, there is also the replica-diagonal order parameter $\bar{q}$. The set of order parameters is completed with m which corresponds to the presence of Mattis states (FE).[21,22] The coupled equations for q_0, q_1, x, $\bar{q}$, and m are solved for several values of degree of frustration a in a phase diagram T versus chemical potential μ. In particular, the RS solution is also obtained when $q_0 = q_1 \equiv q$.

The comparison among the several scenarios displayed in Figs. 1 and 2 elucidates the role of frustration as the essential ingredient responsible for producing naturally inverse freezing in the HFISG model. In other words, an inverse freezing without any need of an artificial entropic advantage. For instance, the comparison between results given in Figs. 1(a) and 1(b) shows that only in the case $a=0.1$ (the strong frustrated regime) a reentrant first-order boundary phase appears. The trivial randomness is not able to generate naturally a reentrance and, therefore, an inverse transition. Furthermore, in Fig. 2, when the level of frustration is diminished, the range in temperature of the SG/PM first-order boundary phase is decreased but, most importantly, the reentrance in this first-order boundary phase is gradually suppressed, what implies in the gradual suppression of inverse freezing until the complete disappearing in the trivial randomness case ($a=0$). Nevertheless, whatever the level of frustration, there is always a reentrance in SG/PM first-order boundary phase which gives an inverse freezing. In contrast, the range of the FE/PM first-order boundary phase is simply increased, nothing else happens. These previous features lead to the conclusion that frustration in any level is the necessary condition to create naturally the entropic advantage of the SG phase as compared with the PM one which generates an inverse freezing. Albeit, these results are restrict to a particular model, we suggest that the role of frustration as an essential ingredient to raise naturally inverse freezing could be more general.

One last remark must be done. The present approach could be used directly in GS model with the coupling J_{ij} as given in Eq. (1) replacing the original Gaussian distributed one.[13] However, the great advantage of the HFISG model is that it would also allow studying the present problem in the presence of a transverse magnetic field Γ.[16,20,33] In Ref. 7, it has been shown that Γ tends to destroy the inverse freezing. Therefore, the presence of an additional Γ would lead to

another question: what would happen with the inverse freezing in the HFISG model when the level of frustration and the strength of quantum effects are simultaneously changed? In that case, it would be possible to investigate the robustness of the inverse freezing by adjusting simultaneously the degree of frustration and Γ. This question is currently under investigation.

ACKNOWLEDGMENTS

APPENDIX A: THE AVERAGE OVER $Z(n)$

In this appendix, the averaging procedure of the partition function of the HFISG model is introduced following closely Ref. 21. The first term in the action A_{SG}^{stat} [see Eq. (12)] can be linearized by a Hubbard-Stratonovich transformation by introducing $n \times p$ auxiliary fields m_ϱ^α which are splitted in two subsets with $n \times (p-l)$ and $n \times l$ terms. Therefore

$$\exp(A_{SG}^{stat}) = \exp\left[-\frac{\beta J p}{2N} \sum_\alpha \sum_i (S_i^\alpha)^2 \right]$$
$$\times \int_{-\infty}^{\infty} Dm_\nu^\alpha \exp\left\{ \tau \sum_{\nu=1}^{l} \sum_\alpha \left[-\frac{1}{2}(m_\nu^\alpha)^2 + \eta_{i,\alpha}^\nu \right] \right\}$$
$$\times \int_{-\infty}^{\infty} Dm_\varrho^\alpha \exp\left\{ \tau \sum_{\varrho=l+1}^{p} \sum_\alpha \left[-\frac{1}{2}(m_\varrho^\alpha)^2 + \eta_{i,\alpha}^\varrho \right] \right\},$$
(A1)

where $\tau = \beta J N$, $\eta_{i,\alpha}^{\nu(\varrho)} = \frac{1}{N}\sum_i \xi_i^{\nu(\varrho)} S_i^\alpha m_{\nu(\varrho)}^\alpha$, and $Dm_{\nu(\varrho)}^\alpha = \Pi_{\nu(\varrho)}\Pi \frac{dm_{\nu(\varrho)}^\alpha}{\sqrt{2\pi}}$.

It is assumed that the relevant contributions come from m_ν^α which are order unity while m_ϱ^α is of order $1/\sqrt{N}$. Therefore, the average over the p-l independent random variables ξ_i^ϱ can be done using $P(\xi_i^\varrho)$ given in Eq. (3) which results in

$$\left\langle\!\!\left\langle \exp\left[\beta J \sum_{\varrho=l+1}^{p} \sum_\alpha \left(\sum_i \xi_i^\varrho S_i^\alpha \right) m_\varrho^\alpha \right] \right\rangle\!\!\right\rangle_\xi$$
$$= \exp\left\{ \sum_i \sum_{\varrho=s}^{p} \ln\left[\cosh\left(\beta J \sum_\alpha S_i^\alpha m_\varrho^\alpha \right) \right] \right\}. \quad (A2)$$

The argument of the exponential in the right-hand side of Eq. (A2) can be expanded up to second order in m_ϱ^α. The result is a quadratic term of the spins variables S_i^α in the last exponential of Eq. (A1). This term can be linearized by introducing the spin-glass order parameter $q_{\alpha\beta}$ using the integral representation of the delta function as

$$\int_{-\infty}^{\infty} \frac{dr'_{\alpha\beta}}{2\pi} \exp\left[ir'_{\alpha\beta}\left(q_{\alpha\beta} - \frac{1}{N}\sum_i S_i^\alpha S_i^\beta \right) \right]$$
$$= \delta\left(q_{\alpha\beta} - \frac{1}{N}\sum_i S_i^\alpha S_i^\beta \right). \quad (A3)$$

Therefore, the exponential involving m_ϱ^α in Eq. (A1) can be written as

$$\exp\left\{ \beta N \sum_{\varrho=l+1}^{p} \sum_\alpha \left[-\frac{1}{2}(m_\varrho^\alpha)^2 + \frac{1}{N}\left(\sum_i \xi_i^\varrho S_i^\alpha \right) m_\varrho^\alpha \right] \right\}$$
$$= \int_{-\infty}^{\infty} \prod_{\alpha\beta} \frac{dq_{\alpha\beta} d\tilde{r}_{\alpha\beta}}{2\pi} \exp\left[\frac{\beta}{2} \sum_{\varrho=l+1}^{p} m_\varrho^\alpha \Lambda_{\alpha\beta} m_\varrho^\beta D_{\alpha\beta} \right]$$
(A4)

with

$$D_{\alpha\beta} = i\sum_{\alpha\beta} \tilde{r}_{\alpha\beta}\left(q_{\alpha\beta} - \frac{1}{N}\sum_i S_i^\alpha S_i^\beta \right), \quad (A5)$$

where the matrix element

$$\Lambda_{\alpha\beta} = (1 - \beta q_{\alpha\alpha})\delta_{\alpha\beta} + \beta q_{\alpha\beta}(1 - \delta_{\alpha\beta}). \quad (A6)$$

Introducing Eqs. (A4)–(A6) into Eq. (A1), the m_ϱ^α fields can be integrated to give

$$\langle\!\langle \exp(A_{SG}^{stat}) \rangle\!\rangle_\xi$$
$$= \exp\left[-\frac{\beta J p}{2N} \sum_i (S_i^\alpha)^2 \right] \left\langle\!\!\left\langle \int_{-\infty}^{+\infty} Dm_\nu^\alpha \right.\right.$$
$$\left.\left. \times \exp\left\{ \tau \sum_{\nu=1}^{l} \sum_\alpha \left[-\frac{1}{2}(m_\nu^\alpha)^2 + \eta_{i,\alpha}^\nu \right] \right\} \right\rangle\!\!\right\rangle_\xi$$
$$\times \int_{-\infty}^{\infty} \prod_{\alpha\beta} \frac{dq_{\alpha\beta}\tilde{r}_{\alpha\beta}}{2\pi} \exp\left\{ D_{\alpha\beta} - \frac{1}{2}(p-l)Tr\ln \underline{\underline{\Lambda}} \right\}. \quad (A7)$$

Assuming $l=1$ in Eq. (A7), the averaged partition function is given as

$$\langle\!\langle Z(n) \rangle\!\rangle_\xi = \int_{-\infty}^{\infty} Dm_1^\alpha \int_{-\infty}^{\infty} \prod_{\alpha\neq\beta} \frac{dq_{\alpha\beta}d\tilde{r}_{\alpha\beta}}{2\pi} \prod_\alpha \frac{dq_{\alpha\alpha}d\tilde{r}_{\alpha\alpha}}{2\pi}$$
$$\times \exp\left[i\sum_\alpha \tilde{r}_{\alpha\alpha}q_{\alpha\alpha} + i\sum_{\alpha\neq\beta} \tilde{r}_{\alpha\beta}q_{\alpha\beta} \right.$$
$$\left. -\frac{\beta J N}{2}\sum_\alpha (m_1^\alpha)^2 \right]$$
$$\times \exp\left[-\frac{p-1}{2}Tr\ln \underline{\underline{\Lambda}} \right] \langle\!\langle \Theta(\tilde{r}_{\alpha\beta},\tilde{r}_{\alpha\alpha},m_1^\alpha) \rangle\!\rangle_\xi, \quad (A8)$$

where the matrix $\underline{\underline{\Lambda}}$ is defined in Eq. (A6) and

$$\Theta(\tilde{r}_{\alpha\beta}, \tilde{r}_{\alpha\alpha}, m_1^\alpha)$$

$$= \prod_\alpha^n \int D(\phi_\alpha^* \phi_\alpha)$$

$$\times \exp\left[A_i^{\alpha_0} + \sum_j \sum_{\sigma\alpha} \sum_\omega \phi_{j\sigma\alpha}^*(\omega) g_j^{-1}(\omega) \phi_{j\sigma\alpha}(\omega) \right]$$

$$(A9)$$

with

$$A_i^{\alpha_0} = -i \sum_{\alpha \neq \beta} \tilde{r}_{\alpha\beta} \left(\frac{1}{N} \sum_i S_i^\alpha S_i^\beta \right) - \sum_\alpha \left(\frac{\beta J p}{2} + i \tilde{r}_{\alpha\alpha} \right) \frac{1}{N} \sum_i (S_i^\alpha)^2$$

$$+ \beta J \sum_\alpha \left(\sum_i \xi_i^1 S_i^\alpha \right) m_1^\alpha \qquad (A10)$$

and $g_j^{-1}(\omega) = i\omega + \beta\mu$. The trace of the matrix $\underline{\underline{\Lambda}}$ given in Eq. (A6) is obtained in terms of its eigenvalues.

The grand canonical potential is found introducing Eq. (A8) in Eq. (10) which is evaluated at the saddle point. Thus

$$-i\tilde{r}_{\alpha\alpha} = \frac{\beta^2 J^2}{2} \langle (m_1^\alpha)^2 \rangle = \frac{\beta^2 J^2}{2} p r_{\alpha\alpha} \qquad (A11)$$

and

$$-i\tilde{r}_{\alpha\beta} = \frac{\beta^2 J^2}{2} \langle (m_1^\alpha m_1^\beta) \rangle = \frac{\beta^2 J^2}{2} p r_{\alpha\beta}; \quad \alpha \neq \beta. \quad (A12)$$

APPENDIX B: TRICRITICAL POINTS

This appendix presents a procedure to obtain the tricritical point (μ_{tc}, T_{tc}) for both cases: $a=0$ and $a>0$. For $a=0$, the Landau expansion of the grand canonical potential, Eq. (19), in powers of m gives

$$\beta\Omega(m) = A_0 + A_2 m^2 + A_4 m^4 + A_6 m^6 + \cdots \quad (B1)$$

with

$$A_2 = \beta J \{1 - (\beta J)/[1 + \cosh(\beta\mu)]\}/2, \qquad (B2)$$

$$A_4 = \beta^4 J^4 [2 - \cosh(\beta\mu)] \operatorname{sech}[(\beta\mu)/2]^4/96. \quad (B3)$$

The tricritical point is obtained when $A_2 = A_4 = 0$. The position of T_{2c} in the Fig. 1(a) for $\mu=0$ can be also checked from the equation $A_2 = 0$.

For $a > 0$, the PM/SG phase transition is investigated. In this case, it is assumed that there is no essential difference between RS and 1S-RSB schemes concerning the location of the tricritical point.[2] Therefore, we start with the thermodynamic potential within the RS solution ($q \equiv q_1 = q_0$, $r \equiv r_1 = r_0$, and $x=0$) written explicitly as a function of the order parameters r and $\bar{r}$, and with $m=0$

$$\beta\Omega = -\beta\mu + \frac{a}{2}\left[\beta J \bar{r} - \frac{r}{r - \bar{r}} - \ln(\bar{r} - r) \right] - \int Dz$$

$$\times \ln[\cosh\beta\mu + e^{[\beta^2 J^2 a/2(\bar{r}-r) - \beta Ja/2]} \cosh\beta J \sqrt{arz}],$$

$$(B4)$$

where r and $\bar{r}$ are given by Eqs. (22) and (24) within the RS solution, respectively.

Equation (B4) is expressed as an expansion in powers of r, which is related to the SG order parameter. Therefore

$$\beta\Omega = \sum_{i=1}^4 f_i(\bar{r}, \mu, T, a) r^i, \qquad (B5)$$

where $\bar{r}(r, \mu, T, a)$ is obtained by a saddle-point solution of Ω. In this case, $\bar{r}(r, \mu, T, a)$ can also be written in the form of a series

$$\bar{r} = \bar{r}_0 + \bar{r}_1 r + \bar{r}_2 r^2 \qquad (B6)$$

with $r_1 = 0$ as a result

$$\bar{r}_0 = [\beta J(1 - \beta J X_0)]^{-1}, \qquad (B7)$$

$$\bar{r}_2 = -\frac{2 + \beta^6 J^6 a^2 \bar{r}_0^3 X_0^2(1 - X_0)}{\bar{r}_0[2 - \beta^4 J^4 a \bar{r}_0^2 X_0(1 - X_0)]} \qquad (B8)$$

and

$$X_0 = \frac{\exp\left(\dfrac{\beta^2 J^2 a \bar{r}_0}{2}\right)}{e^{\beta Ja/2} \cosh\beta\mu + \exp\left(\dfrac{\beta^2 J^2 a \bar{r}_0}{2}\right)}. \qquad (B9)$$

Now, Eq. (B6) is introduced into the coefficients of expression (B5), which are expanded in powers of r again. The resulting expression is then expressed in powers of the SG order parameter q by expanding r

$$\beta\Omega = F_0 + \frac{F_2 q^2}{(1 - \beta J \bar{q}_0)^4} + \frac{F_3 q^3}{(1 - \beta J \bar{q}_0)^6} + \frac{F_4 q^4}{(1 - \beta J \bar{q}_0)^8}$$

$$(B10)$$

with

$$F_2 = \frac{a}{4}\left(\beta^4 J^4 a X_0^2 - \frac{1}{\bar{r}_0^2} \right), \qquad (B11)$$

$$F_3 = \frac{a}{3}\left(\beta^6 J^6 a^2 X_0^3 + \frac{1}{\bar{r}_0^3} \right), \qquad (B12)$$

$$F_4 = \frac{a}{4}\left\{ \frac{\beta^4 J^4 a^2 \bar{r}_2}{2}(X_0 - X_0^2)(\bar{r}_2 + 2\beta^2 J^2 a X_0) \right.$$

$$\left. + \frac{\beta^8 J^8 a^3 X_0^2}{12}(45 X_0^2 - 12 X_0 + 1) \right\} - \frac{1}{\bar{r}_0^4}\left[(\bar{r}_0 \bar{r}_2 - 1)^2 + \frac{1}{2} \right]$$

$$- 6\beta J(1 - \beta J \bar{q}_0) F_3, \qquad (B13)$$

where $\bar{q}_0 = 1/[\beta J(1 + \sqrt{a})]$. The PM/SG second-order phase transition occurs when $F_2 = 0$ and $F_4 > 0$ with the tricritical point located when $F_2 = 0$ and $F_4 = 0$. In particular, one can use the condition $F_2 = 0$ with Eqs. (B7) and (B9) to obtain the critical temperature T_{2f} by solving

$$\cosh\beta_{2f}\mu = \exp\left(\frac{J\beta_{2f}\sqrt{a}}{2} \right)[J\beta_{2f}(1 + \sqrt{a}) - 1], \quad (B14)$$

where $\beta_{2f} = 1/T_{2f}$. For $\mu = 0$, it is recovered the result $T_{2f} = 0.729$ for $a = 0.1$

APPENDIX C: FIRST-ORDER TRANSITION AT ZERO TEMPERATURE

Here a procedure is presented to obtain the first-order boundary phases of FE/PM phases ($a=0$) and SG/PM phases ($a>a_c$) at $T=0$ within the RS and 1S-RSB solutions. For $a=0$, the grand canonical potential of FM solution at $T=0$ is $\Omega_{fm}=-\mu-\frac{J}{2}$. By comparing Ω_{fm} with the grand potential of PM phase, $\Omega_{\mathrm{PM}}=-2\mu$, the first-order boundary is located at $\mu=0.5J$. For the cases shown in Fig. 2, it is recovered the grand canonical potential for $a=0$.

For $a>a_c$, the effects of frustration are dominants. In this case for RS solution, $\bar{q}-q \propto T$ for $T \to 0$. Therefore, close to the transition, which means $\mu/J > \frac{a\beta J(\bar{q}-q)}{2[1-\beta J(\bar{q}-q)]}$, the Ω_{SG} at $T=0$ is

$$\Omega_{\mathrm{SG}} = -2\mu + \sqrt{2ar}\left[y\,\mathrm{erfc}\left(\frac{y}{\sqrt{2}}\right) - \frac{e^{-y^2/2}}{\sqrt{2\pi}}\right], \qquad \text{(C1)}$$

where $\mathrm{erfc}(z)=1-\mathrm{erf}(z)$ [$\mathrm{erf}(z)$ is the error function], $y \equiv \frac{1}{\sqrt{ar}}\left(\mu/J - \frac{a}{\sqrt{2\pi ar}\,e^{y^2/2}-2}\right)$ and $r=\mathrm{erfc}(\frac{y}{\sqrt{2}})$. From the condition $\Omega_{\mathrm{SG}}=\Omega_{\mathrm{PM}}$, y and r can be solved which allows finding $\mu_{1f}(T=0)$. Particularly, $\mu_{1f}(T=0)=0.689$ for $a=0.1$.

In 1S-RSB scheme, for $T \to 0$, $\chi \equiv \beta J(\bar{q}-q_1)$ is independent of T and $x=\gamma T/J$. Therefore, close to the transition, where $\mu/J > \frac{a\beta J(\bar{q}-q_1)}{2[1-\beta J(\bar{q}-q_1)]}$, the Ω_{SG} at $T=0$ is

$$\Omega_{\mathrm{SG}} = \frac{Ja}{2}\left\{\bar{r}\chi + \frac{q_1}{1-\chi} + \gamma(r_1 q_1 - r_0 q_0) - \frac{q_0}{1-\chi-\gamma(q_1-q_0)} \right.$$
$$\left. + \frac{1}{\gamma}\ln\left[\frac{1-\chi-\gamma(q_1-q_0)}{(1-\chi)}\right]\right\} - 2\mu - \frac{J}{\gamma}\int Dz\,\ln\frac{I(z)}{2},$$
$$\text{(C2)}$$

where

$$I(z) = e^{\gamma\vartheta_+}\left\{1+\mathrm{erf}\left[\frac{\eta_+}{\sqrt{2a(r_1-r_0)}}\right]\right\}$$
$$+ e^{\gamma\vartheta_-}\left\{1+\mathrm{erf}\left[\frac{\eta_-}{\sqrt{2a(r_1-r_0)}}\right]\right\} + \mathrm{erf}\left[\frac{\bar{u}+\sqrt{ar_0}z}{\sqrt{2a(r_1-r_0)}}\right]$$
$$+ \mathrm{erf}\left[\frac{\bar{u}-\sqrt{ar_0}z}{\sqrt{2a(r_1-r_0)}}\right]$$
$$\text{(C3)}$$

with $\eta_\pm = \pm\sqrt{ar_0}z + a\gamma(r_1-r_0)-\bar{\mu}$, $\bar{\mu}=\mu/J-\frac{a}{2}\frac{\chi}{1-\chi}$, and $\vartheta_\pm = \pm\sqrt{ar_0}z+\frac{a}{2}\gamma(r_1-r_0)-\bar{\mu}$. The previous results for RS solution are recovered from Eqs. (C2) and (C3) when $q \equiv q_1 \equiv q_0$. Again, equations for χ, q_0, q_1, r_0, r_1, and γ can be obtained from Ω_{SG} and solved. In this case, $\mu_{1f}(T=0)=0.682$ for $a=0.1$.

---

*ggarcia@ccne.ufsm.br

[1] N. Schupper and N. M. Shnerb, Phys. Rev. E **72**, 046107 (2005); Phys. Rev. Lett. **93**, 037202 (2004).

[2] A. Crisanti and L. Leuzzi, Phys. Rev. Lett. **95**, 087201 (2005).

[3] M. Sellitto, Phys. Rev. B **73**, 180202(R) (2006).

[4] S. Prestipino, Phys. Rev. E **75**, 011107 (2007).

[5] L. Leuzzi, Philos. Mag. **87**, 543 (2007).

[6] R. Angelini, G. Ruocco, S. De Panfilis, Phys. Rev. E **78**, 020502(R) (2008).

[7] S. G. Magalhaes, C. V. Morais, and F. M. Zimmer, Phys. Rev. B **77**, 134422 (2008).

[8] A. L. Greer, Nature (London) **404**, 134 (2000).

[9] O. Portmann, A. Vaterlaus, and D. Pescia, Nature (London) **422**, 701 (2003).

[10] N. Avraham, Boris Khaykovich, Yuri Myasoedov, Michael Rappaport, Hadas Shtrikman, Dima E. Feldman, Tsuyoshi Tamegai, Peter H. Kes, Ming Li, Marcin Konczykowski, Kees van der Beek, and Eli Zeldov, Nature (London) **411**, 451 (2001).

[11] M. R. Feeney, P. G. Debenedetti, and F. H. Stillinger, J. Chem. Phys. **119**, 4582 (2003).

[12] M. Blume, Phys. Rev. **141**, 517 (1966); H. W. Capel, Physica (Amsterdam) **32**, 966 (1966).

[13] S. K. Ghatak and D. Sherrington, J. Phys. C **10**, 3149 (1977).

[14] E. Fradkin, B. A. Huberman, and S. H. Shenker, Phys. Rev. B **18**, 4789 (1978).

[15] R. Oppermann and A. Muller-Groeling, Nucl. Phys. B **401**, 507 (1993).

[16] A. Theumann, A. A. Schmidt, and S. G. Magalhães, Physica A **311**, 498 (2002).

[17] W. Wiethege and D. Sherrington, J. Phys. C **19**, 6983 (1986).

[18] I. P. Castillo and D. Sherrington, Phys. Rev. B **72**, 104427 (2005).

[19] H. Feldmann and R. Oppermann, J. Phys. A **33**, 1325 (2000).

[20] F. M. Zimmer and S. G. Magalhaes, Phys. Rev. B **74**, 012202 (2006).

[21] D. J. Amit, *Modeling Brain Function: The World of Attractor Neural Networks* (Cambridge University Press, Cambridge, England, 1989).

[22] D. J. Amit, H. Gutfreund, and H. Sompolinsky, Phys. Rev. A **32**, 1007 (1985).

[23] D. J. Mattis, Phys. Lett. A **56**, 421 (1976).

[24] J. P. Provost and G. Vallee, Phys. Rev. Lett. **50**, 598 (1983).

[25] D. Sherrington and S. Kirkpatrick, Phys. Rev. Lett. **35**, 1792 (1975); S. Kirkpatrick and D. Sherrington, Phys. Rev. B **17**, 4384 (1978).

[26] A. J. Bray and M. A. Moore, J. Phys. C **13**, L655 (1980).

[27] G. Parisi, J. Phys. A: Math. Gen. **13**, 1101 (1980).

[28] A. Theumann and M. Vieira Gusmão, Phys. Lett. A **105**, 311 (1984).

[29] J. Miller and D. A. Huse, Phys. Rev. Lett. **70**, 3147 (1993).

[30] F. A. da Costa, C. S. O. Yokoi, and S. R. A. Salinas, J. Phys. A **27**, 3365 (1994).

[31] P. Mottishaw, Europhys. Lett. **1**, 409 (1986).

[32] J. W. Negele, H. Orland, *Quantum Many-Particle Systems* (Addison-Wesley, EUA, 1988).

[33] F. M. Zimmer and S. G. Magalhães, Physica A **359**, 380 (2006).

[34] D. J. Amit, H. Gutfreund, and H. Sompolinsky, Ann. Phys. **173**, 30 (1987).